

# Estimating Eddy-Induced Heat Transport by Combining Satellite Altimetry, Argo, and TMI Measurements

Bo Qiu and Shuiming Chen (bo@schcn@soest.hawaii.edu), Department of Oceanography, University of Hawaii aii, Honolulu, HI, 96822, USA

## 1. Introduction

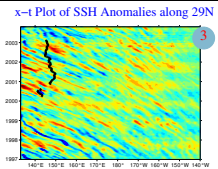
Many studies in the past have investigated the ocean's role in closing the global heat balance and a consensus has emerged that the time-mean ocean circulation carries about one-third to one-half of the excess heat from the tropics to the poles. With the ocean being a turbulent medium in which the time-mean circulation is in general much weaker than its time-varying signals, several recent studies have started to look into the heat transport carried by mesoscale eddies of the ocean (e.g. Holloway 1986; Stammer 1998; Roemmich and Gilson 2001; Wunsch 1999).

With new observational ability to measure mesoscale eddy activity becoming available in recent years, we attempt in this study to re-evaluate the eddy heat transport in the North Pacific. In contrast to the studies by Holloway (1986) and Stammer (1998) in which satellite altimetry data were used to derive the statistical properties of the mesoscale eddy field, the satellite SSH data will be used in this study to evaluate the movement and strength of individual mesoscale eddies. In addition to the satellite altimetry data, we will also in this study utilize the sea surface temperature (SST) data measured by the Tropical Rainfall Measuring Mission (TRMM) Microwave Imager and the in-situ temperature and salinity data from the global Argo float program (Fig. 1; right).

These two data sets have become available recently and, as we will show below, provide us with an effective means to capture the thermal structures of the mesoscale eddies. By combining the concurrent temperature and surface dynamic height direct measurements, we seek to estimate the eddy heat flux  $v'T'$  directly.

## 2. Structures of Mesoscale Eddies

Figures 2b and 2c show the  $T(z)$  and  $S(z)$  profiles measured by Argo float 29033 (See Fig. 2a for its trajectory). Figures 2d and 2e show the  $T(z)$  and  $S(z)$  anomaly profiles after removing the climatological  $T/S$  values of WOA01. The profiles capture the procession of westward propagating warm- and cold-core eddies (see Fig. 3; right).



A noticeable feature in Fig. 2d is that the  $T(z)$  anomalies in the surface layer tend to precede those in the main thermocline (see Fig. 4b). With the satellite altimetric data providing the full time-varying SSH field, it is possible to identify the locations of the float relative to the mesoscale eddies. For example, Fig. 5 shows the sequence of the SSH anomaly field from March 11 to May 29, 2001, during which a westward-translating warm-core eddy passed by the profiling float. Using the information of Fig. 5, we can plot the float-derived  $T'(z)/S'(z)$  profile in a reference frame moving with the eddy and calculate the eddy-induced eddy heat transport (Fig. 6; top panel). Similar calculation is done for a cold-core eddy shown in Fig. 6, bottom panel. For both of the warm- and cold-core eddies shown in Fig. 6, poleward eddy heat transport is mostly confined to the surface 200 m layer.

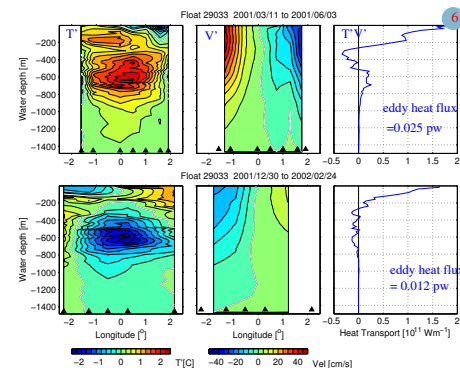
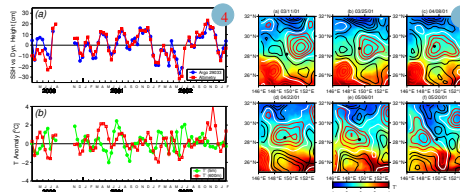
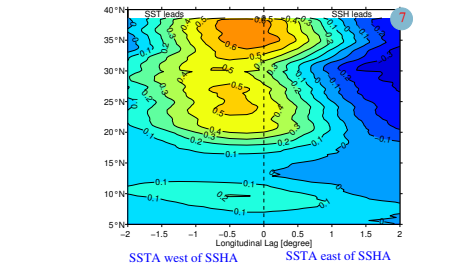


Figure 7 shows longitudinal lag correlation between the SSH and SST anomalies in the western North Pacific (130°E – 170°W). A negative (positive) lag here indicates a warm SST anomaly being located to the west (east) of a high SSH anomaly. Consistent with the Argo measurements, warm (cold) SST anomalies are found to be located to the west of high (low) SSH anomalies.

Lagged Correlation between TMI SSTA and AVISO SSHA



## 3. Eddy Heat Transport in N Pacific

Confinement of eddy heat transport to the seasonal thermocline suggests an effective depth  $H_e$  may be sought that relates the surface and depth-integrated eddy heat transport values:

$$H_e = \frac{\int_0^{500\text{dbar}} v'T'(z) dz}{v'T'|_{z=0}}$$

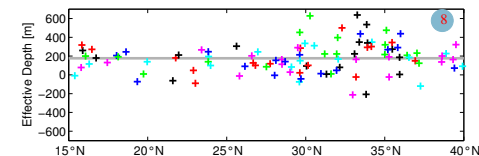
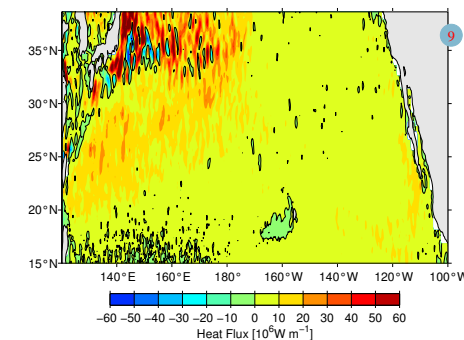


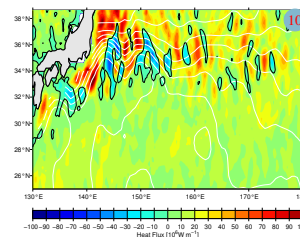
Figure 8 (above) shows the effective depth  $H_e$  values estimated from the 102 Argo floats in the subtropical North Pacific, and plotted as a function of the central latitude of each float's trajectories. The overall mean value is  $\bar{H}_e = 177$  m.

Using this conversion value, Fig. 9 (below) shows the estimated meridional eddy heat flux transport ( $\rho_0 T' v' H_e$ ) in the subtropical North Pacific, based on the 6-yr concurrent altimetric SSH and TMI SST data. Fig. 10 (below) is for the Kuroshio Extension region.

Meridional Eddy Heat Transport in the Subtropical North Pacific

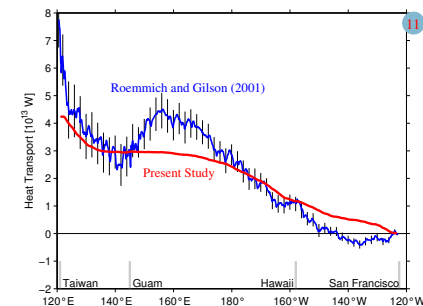


Eddy Heat Transport near the Kuroshio Extension



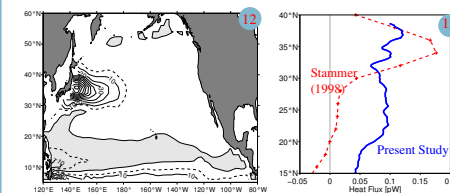
## 4. Major Findings

A. Large poleward eddy heat transport is found in the central North Pacific along the SW-NE tilting band of the Subtropical Front. This high transport band is also found in the study by Roemmich and Gilson (2001) and our estimate compares well with the Roemmich and Gilson's results using the high-resolution XBT/XCTD transect of San Francisco – Honolulu – Guam – Taiwan (see Fig. 11; below). The large eddy heat transport is the consequence of baroclinic instability due to the vertical shear of the terminal mean zonal flows (Qiu 1999).



B. In the Kuroshio Extension region, the meandering zonal jet is found to generate oppositely signed eddy heat fluxes (see Fig. 10). As a result, the zonally integrated poleward heat transport associated with the Kuroshio Extension is at a level of  $O(0.1 \text{ pw})$ , smaller than the previous estimates based on turbulent closure schemes by Stammer (1998) (Figs. 12 and 13; below).

Meridional Eddy Heat Transport by Stammer (1998) Zonal Average Flux (pw)



## References and Acknowledgment

Holloway, G., 1986. *Nature*, 323, 243–244.  
 Qiu, B., 1999. *JPO*, 29, 2471–2486.  
 Roemmich, D., and J. Gilson, 2001. *JPO*, 31, 675–687.  
 Stammer, D., 1998. *JPO*, 28, 727–739.  
 Wunsch, C., 1999. *JGR*, 104, 13,235–13,249.  
 The Argo float data was provided by the USGODAE Global Data Assembly Center, the TMI data by Remote Sensing Systems, and the merged T/P and ERS-1/2 altimeter data by the CLS Space Oceanography Division as part of the Environment and Climate EU ENACT project. This study was supported by NASA through Contracts 1207881 and 1228847.

For preprints, please visit <http://www.soest.hawaii.edu/oceanography/bo>